Science and Technology for Energy Transition **79**, 90 (2024)

https://doi.org/10.2516/stet/2024087

Available online at:
stet-review.org

Emerging Advances in Hybrid Renewable Energy Systems and Integration
Muhammad Zakarya, Santosh Tirunagari, Jinguang Han and Peiying Zhang (Guest Editors)

Regular Article — Open Access

Comparative analysis of various nanomaterials mixed with WCO biodiesel on CI engine's performance and emissions

Altaf Hussain Bagawan and Syed Abbas Ali*

[1] Department of Mechanical Engineering, SECAB Institute of Engineering and Technology, Vijaypur, 586109, Karnataka, India

Received: 10 July 2024 / Accepted: 25 September 2024

Abstract. The experimental investigations of performance and emission parameters of a compression ignition (CI) engine run by waste cooking oil (WCO) biodiesel dispersed with nanomaterials. The nanomaterials, Cerium oxide, Magnesium oxide, and Aluminium oxide of 30 ppm and 40 ppm dosages are mixed with the 20% of WCO biodiesel and diesel using an ultrasonicator. The performance and emission parameters are investigated by running the CI engine at constant speed for different loads. Based on the conducted experiments, it has been observed that the improvement in performance emission characteristics of CI engines is due to the addition of Cerium oxide, Magnesium oxide, and Aluminium oxide nanomaterials at 30 ppm and 40 ppm dosages of 20% WCO nanoparticles compared with that of diesel. It can therefore be concluded that adding nanomaterials in higher doses enhances CI engine performance and emissions.

Keywords: Cerium oxide, Magnesium oxide, Aluminium oxide, Waste cooking oil, Emissions, Performance.

1 Introduction

The most advantageous in the vehicular engine era is biodiesel, as it can become a substitute for fuel for engines [1–4]. The work carried out so far on biodiesel preparation, examination of performance variables, and combustion-emission characteristics of engines has become the topic of interest in the last few decades [1, 2, 4–7]. One of the most crucial factors in reducing production costs is recognized to be the cost of biodiesel, which is still more expensive than diesel and hence prevents its commercial adoption [8]. It is recognized that close to 60–70% of the total production cost of biodiesel is due to the feedstock (raw material) used. Waste cooking oil (WCO), often described as a cost-effective feedstock, is more appealing owing to its favourable cost [5–8]. A lot of work carried out on producing alternate fuel using WCO for many years [5–8]. The study and analysis of CI engines operated with various biodiesel connected to performance, combustion and emission variables have been done in the literature [8–10]. Further, nanomaterial dispersed fuel has been an attraction for many researchers attaining good performance since it reveals the strengthening mechanical, thermophysical chemical properties, performance, combustion, and emission phenomena of traditional materials [11–16]. The complete review of the effect of various nanomaterials on the various parameters of the CI engine has been highlighted in [12]. Work has been done to figure out how Multi-Walled Carbon Nanotube (MWCNT) additions affect WCO biodiesel, and artificial neural networks have been employed to predict emissions [2]. The influence of cerium oxide and magnesium oxide nanoparticles (30 ppm) in WCO biodiesel on engine thermal performance characteristics has appeared in [8]. The nitromethane-Jatropha biodiesel in [1] and nano TiO_2 additives in palm oil-based biodiesel in [13]. Prabhu highlighted the influence of Al_2O_3 and CeO_2 mixed in jatropha-biodiesel [14]. MgO (30–50 ppm) impact on CI engine parameters operated with WCO as experimented in [5]. The research work related to the experimental investigation of oxygenated additives' impact [17] on performance, combustion, and emissions of CI engines run via WCO-biodiesel blends. The consideration of biodiesel (Castor oil) utilizing CeO_2 additives in [18], terebinth oil biodiesel with TiO_2 [19], aquatic fern oil with SiO_2 [20], Chicken waste biofuel with CNT and MnO [21], seed oil [22], poppy seed oil biodiesel [23] for the CI engine analysis. A review on the importance of machine learning and artificial intelligence for optimizing the efficiency of the engine has been thoroughly discussed in [24]. Further, the amount of WCO available in any country is enormous per year, why because the usage of vegetable oil is expanded since few years [25]. The percentage of vegetable oil used in homes and restaurants is the highest. There is not much of the low-cost feedstock WCO has utilized in the literature. Furthermore, the combination of WCO biodiesel-oxide nanoparticles at varying doses to examine the performance and emissions of CI

* Corresponding author: syed.abbasali86@gmail.com

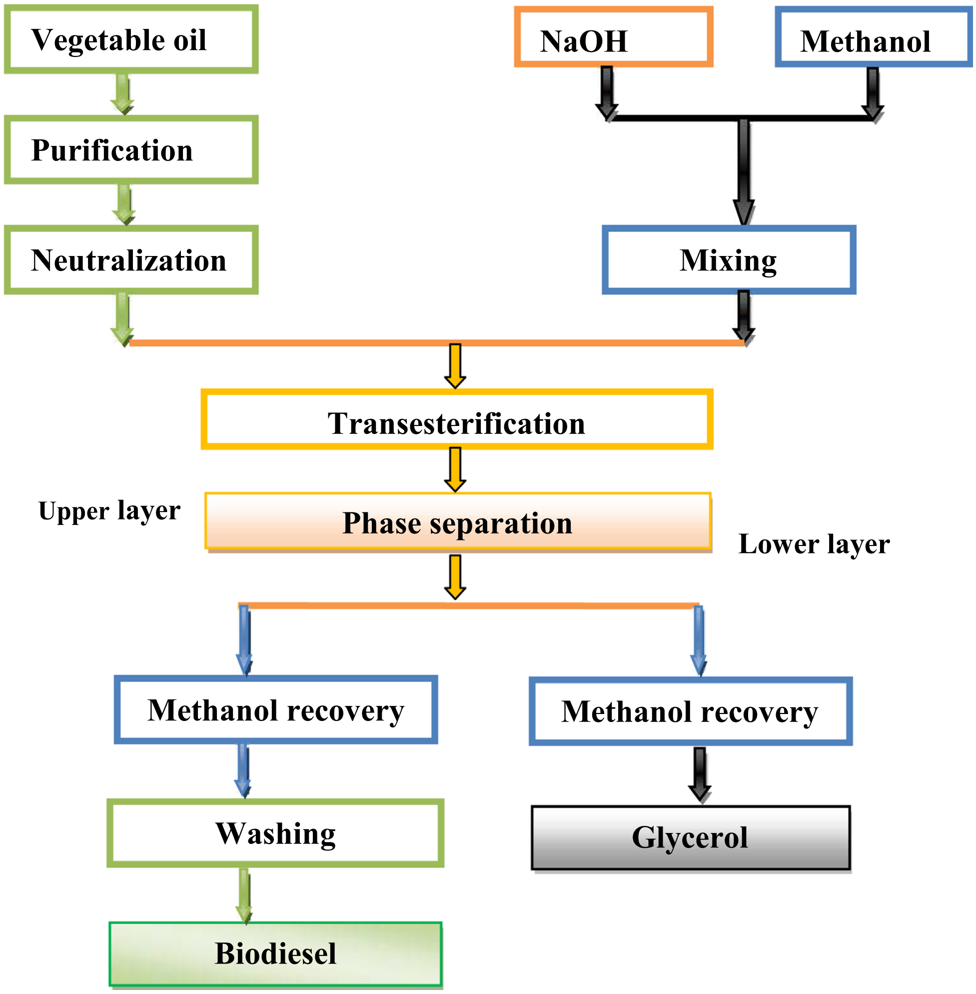

Fig. 1. Block diagram for biodiesel production.

engines is also limited by the comparative study. In keeping with this idea, the current study focuses on an experimental examination to see how different dosages of cerium oxide (CeO_2), magnesium oxide (MgO), and aluminium oxide (Al_2O_3) affect the performance as well as emissions of CI engines.

2 Methods, materials, and experimental set up

2.1 Preparation of biodiesel through transesterification process

The waste cooking oil has been collected from restaurants, corner shops, cafeterias, catering services, and food industries located near the city. The steps to be followed to produce the biodiesel from waste cooking oils are as given in Figures 1 and 2.

2.2 Nanomaterials

The cerium oxide (CeO_2), magnesium oxide (MgO), and aluminium oxide (Al_2O_3) used in this work, as they possess excellent catalytic properties, high thermal stability, enhanced lubrication properties, and a strong redox reaction [26–30], are procured from "Platonic Nano Tech" Pvt. Ltd., India. The X-Ray Diffraction (XRD) instrument is equipped with a Cu Kα X-ray source at 40 kV (Voltage) and 30 mA (Current), a high-resolution detector, data collection over a 2θ range of 10°–90° with an interval of 0.02°. The Transmission Electron Microscopy (TEM) instrument is operated at 200 kV (acceleration voltage), a high-angle annular dark field detector, and has a magnification range from 50,000× to 1,000,000×. Further, the fuel blends containing nanoparticles with high levels of doping might result in early ignition. In addition, these nanoparticles are discharged into the atmosphere as smoke during the engine combustion process, resulting in significant air pollution and possible challenges with vaporization and atomization, as well as increased wear and tear on the surfaces. Lower doses may not be sufficient to achieve better atomization or improved combustion [29, 30]. With this consideration in mind, the authors set limits of 30 ppm and 40 ppm in the present study. Further, the scientific specifications are reported in Table 1. The picture of XRD for CeO_2, MgO, and Al_2O_3 is given in Figures 3–5, and TEM analyses of

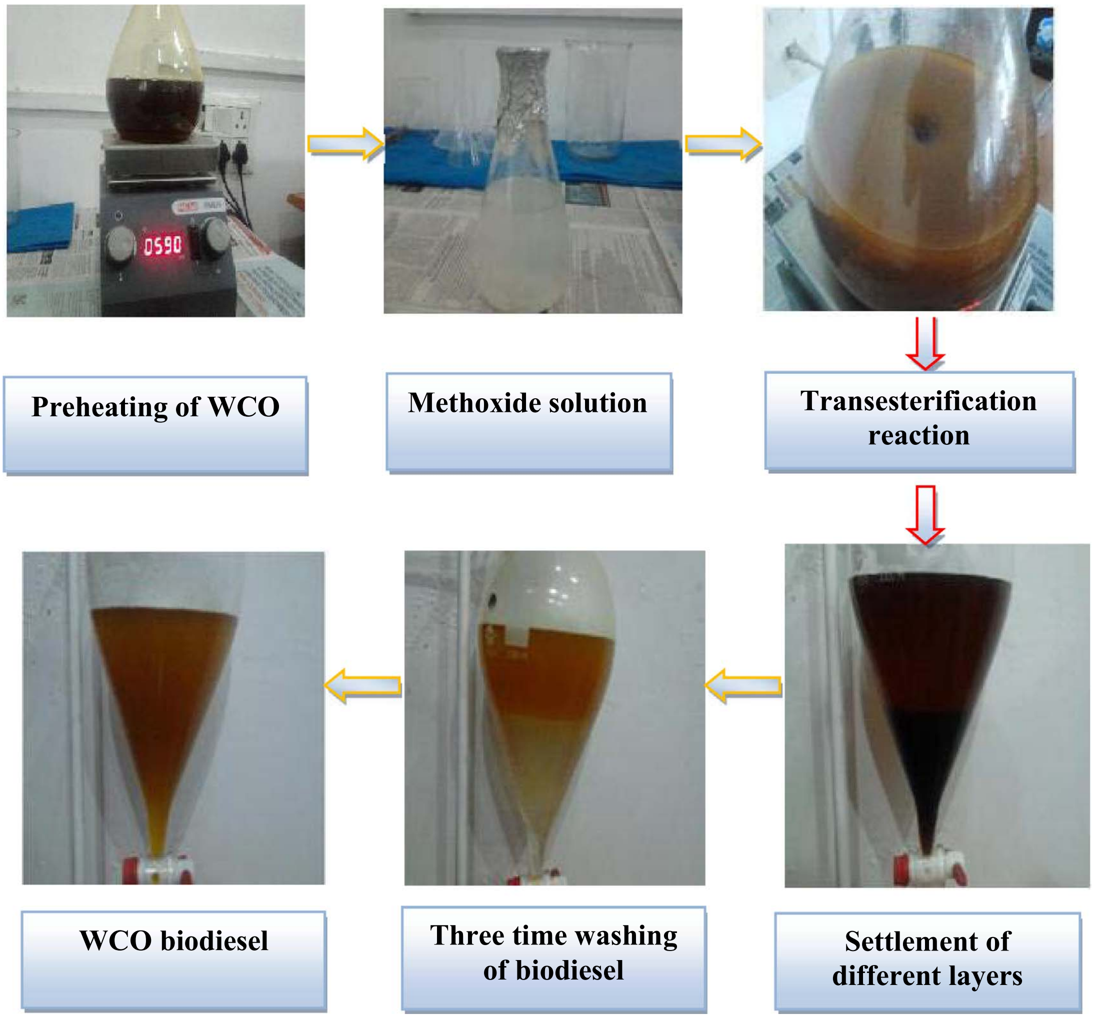

Fig. 2. Biodiesel production process.

CeO_2, MgO, and Al_2O_3 are given in Figures 6–8, respectively. From Figures 3 and 6, it is depicted that, despite being crystalline due to sharp edges, Cerium oxide (CeO_2) material shape is spherical and size ranges from 30 to 50 nm. From Figures 4 and 7, it is seen that amorphous in nature magnesium oxide (MgO) materials are spherical and sizes between 30 and 60 nm. From Figures 5 and 8, it is revealed that, despite being amorphous due to its full width and small half maxima, the aluminium oxide (Al_2O_3) material's shape is spherical, particles are agglomerated, and the size ranges 30–50 nm.

2.3 Ultrasonication: mixing of MWCNT in WCO biodiesel

To promote uniformity of mixture (nanomaterial in biodiesel), many methods have been reported in [31]. The ultrasonic method is capable of efficiently breaking down the nanomaterial agglomerates increasing the stability and improving the dispersion of nanoparticles in the fuel [32]. In the current investigation, an ultrasonication technique is used to mix the nanomaterials in the diesel and biodiesel blend, in which ultrasonic cavitation takes place, which produces shear forces that break up the particle agglomerates and maintain uniformity. Further, the equipment used are shown in Figure 9.

2.4 Experimental investigations of properties of diesel and CeO_2, MgO, Al_2O_3 dispersed WCO biodiesel blends

Blend-B20 is added with CeO_2, MgO, and Al_2O_3 and has been exhibited to acquire the values of calorific value (CV) in kJ/kg, density in kg/m^3, viscosity in cSt, and flash-fire point in degree Celsius using the instruments given in Table 2. Furthermore, the CeO_2, MgO, and Al_2O_3 added WCO-biodiesel blends and diesel properties for 30 ppm and 40 ppm have been discussed in Tables 3–5 and denoted as B20C30, B20M30, B20A30, B20C40, B20M40, and B20A40.

2.5 Test set-up of engine

Figures 10a and 10b represent the image of the engine test rig, and instrumentation part, respectively. The 4-stroke one-cylinder engine is used in this work, operated at

Table 1. Scientific specification of nanomaterials.

S. No.	Scientific specifications	CeO_2	MgO	Al_2O_3
1.	Molecular weight	172.11 g/mol	165.1 g/mol	101.96 g/mol
2.	Particle size	30–50 nm	30–60 nm	30–50 nm
3.	Molecular formula	CeO_2	MgO	Al_2O_3

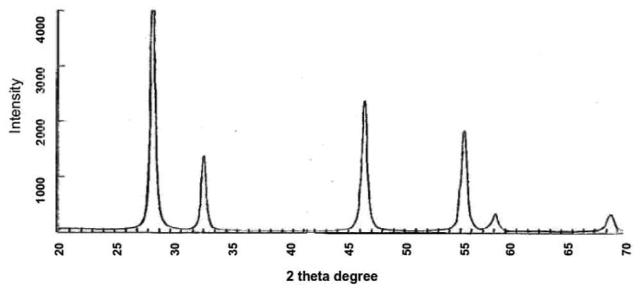

Fig. 3. XRD picture of Cerium oxide.

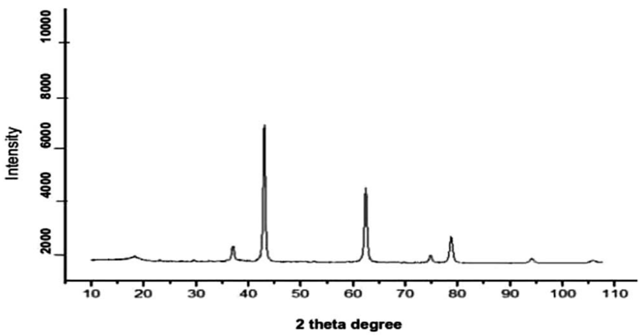

Fig. 4. XRD picture of Magnesium oxide.

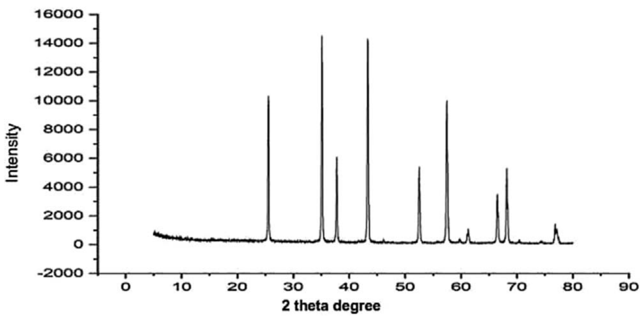

Fig. 5. XRD picture of Aluminum oxide.

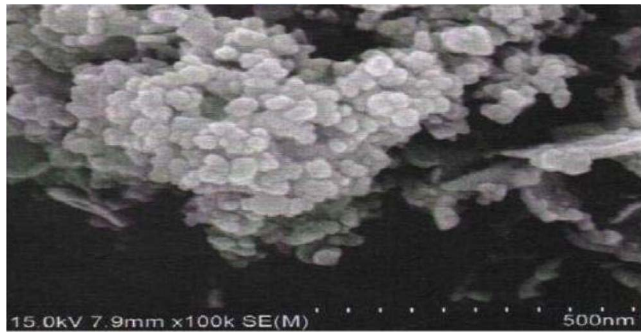

Fig. 6. TEM picture of Cerium oxide.

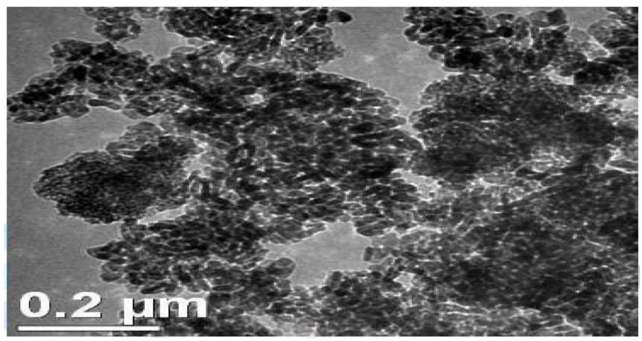

Fig.7. TEM picture of Magnesium oxide.

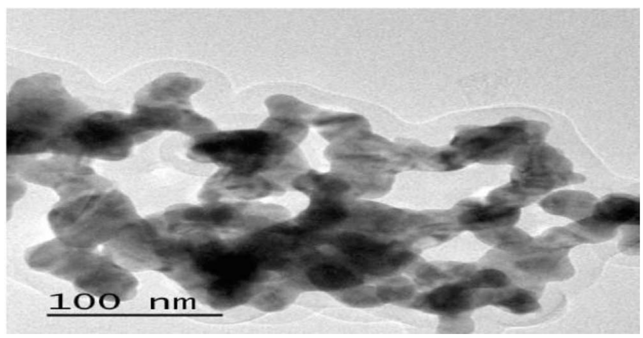

Fig. 8. TEM picture of Aluminum oxide.

constant speed, which is operated at 1500 rpm. The engine is joined with the dynamometer (eddy type). The assessment of air flow – fuel flow employed through transmitters. The load cell is installed to load the engine. The calibrated sensors (pressure) are positioned in the engine to acquire the cylinder pressure. Further, the emission parameters for overall operating conditions are obtained through an emission analyzer (Fig. 11).

2.6 Uncertainty of experimental results

An uncertainty of the different parameters has been conducted to minimize the errors related to the instruments. The instrument's uncertainty relies on the operational and surrounding conditions and accuracy associated with the instrument [2, 3, 11]. In this, multiple tests are performed over and over, and average values are adopted for

(a) (b)

Fig. 9. Equipment used for the mixing of nanomaterials with biodiesel. a) Sonicator; b) Magnetic stirrer.

Table 2. Instruments used for the measurement of fuel properties.

S. No.	Properties	Equipment used	Make model
1.	Calorific value	Digital Bomb Calorimeter	HAMCO, 6B, Sr.190621
2.	Density	Hydrometer	Leimco, M50 SP
3.	Viscosity	Kinematic Viscosity Bath	HAMCO, 48H2STD6, Sr.190623
4.	Flash point	Cleveland's Apparatus	Biological Enterprises, 2005
5.	Fire point	Cleveland's Apparatus	Biological Enterprises, 2005

Table 3. Fuel properties of WCO biodiesel (B20) with CeO_2 and diesel.

S. No.	Properties	Pure diesel (B0)	WCO biodiesel (B20) + CeO_2	
			30 ppm	40 ppm
1.	Calorific value	44,000	43,000	42,500
2.	Density	832	850	860
3.	Viscosity	2.27	2.6	2.7
4.	Flash point	69	61	65
5.	Fire point	53.4	68	72

Table 4. Fuel properties of WCO biodiesel (B20) with MgO and diesel.

S. No.	Properties	Pure diesel (B0)	WCO biodiesel (B20) +MgO	
			30 ppm	40 ppm
1.	Calorific value	44,000	43,555	42,900
2.	Density	832	851	859
3.	Viscosity	2.27	2.7	2.75
4.	Flash point	69	58	65
5.	Fire point	53.4	67	71

Table 5. Fuel properties of WCO biodiesel (B20) with Al_2O_3 and diesel.

S. No.	Properties	Pure diesel (B0)	WCO biodiesel (B20) $+Al_2O_3$	
			30 ppm	40 ppm
1.	Calorific value	44,000	43,100	42,888
2.	Density	832	862	865
3.	Viscosity	2.27	2.6	2.68
4.	Flash point	69	65	68
5.	Fire point	53.4	69	73

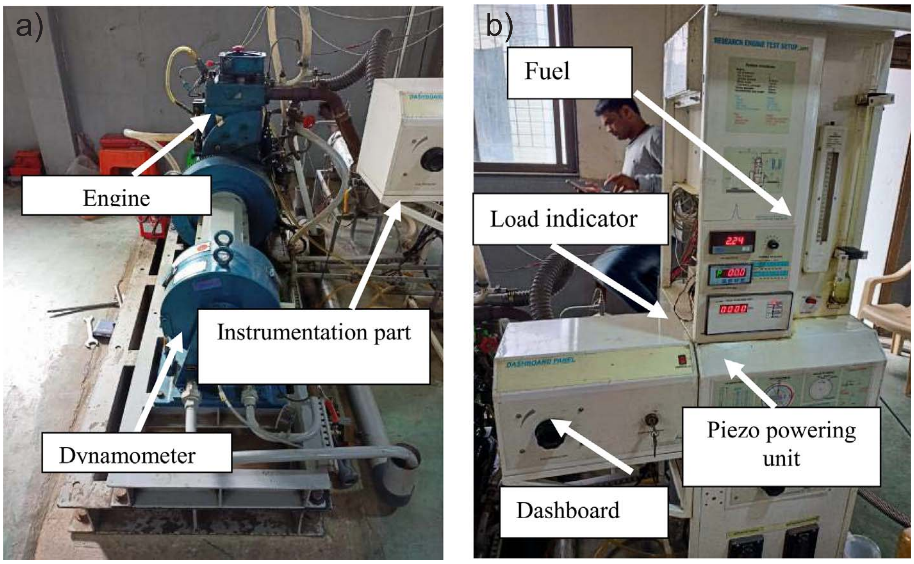

Fig. 10. Photograph of a) Engine test rig and b) Instrumentation part.

subsequent analysis (Table 6). The percentage error in brake thermal efficiency (BTE), specific fuel consumption (SFC), mechanical efficiency (η), unburnt hydrocarbons or hydrocarbons (HC), carbon monoxide (CO), oxides of nitrogen or nitrogen oxide (NO_x), Smole opacity, calorific value (CV), viscosity, density, and flash/fire point is 1%, 2%, 1%, 0.1%, 0.01%, 1%, 3%, 1%, 0.5%, 2%, and 1%, respectively. The following expression is used to compute the total percentage uncertainty of the present experimental study and it is within the reasonable limit.

3 Results and discussions

An experimental investigation has been employed using a CI engine with a load from 2.5 kg to 10 kg including an interval of 2.5 kg using CeO_2, MgO, and Al_2O_3 nanomaterial (30 ppm and 40 ppm) mixed in WCO biodiesel-B20 blend and diesel. The performance parameters examined are BTE, SFC, and mechanical efficiency (η). Furthermore, the emissions under investigation are CO, HC, NO_x, and smoke opacity.

$$\text{Total uncertainity} = \sqrt{\left((\text{BTE})^2 + (\text{SFC})^2 + (\eta)^2 + (\text{HC})^2 + (\text{CO})^2 + (\text{NO})^2 + (\text{Smole})^2 + (\text{CV})^2 + (\text{Viscosity})^2 + (\text{Density})^2 + (\text{Flas/Fire point})^2\right)}$$

$$\text{Total uncertainity} = \sqrt{\left((1)^2 + (2)^2 + (1)^2 + (0.1)^2 + (0.01)^2 + (0.1)^2 + (3)^2 + (1)^2 + (0.5)^2 + (2)^2 + (1)^2\right)} = \pm 4.61\%.$$

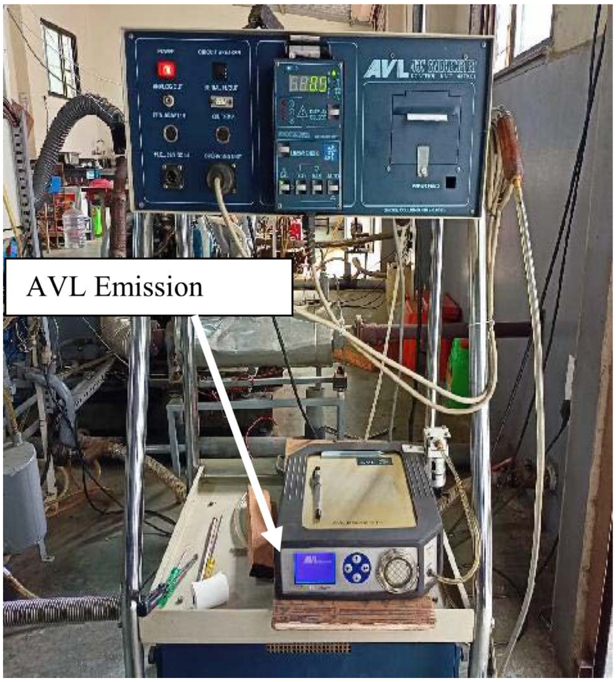

Fig. 11. Photograph of emission analyzer.

Table 6. Uncertainty of experimental results.

Details	Resolution
HC (range)	1 parts per million
CO (range)	0.001% Volume
NO_x (range)	1 parts per million – Volume
CO_2	0.1% Volume
Load indicator	0.2 bar
Crank angle sensor	1°
Calorimeter	1% kJ/kgK
Viscometer	0.5 cSt
Flash and fire point	1°

3.1 Influence of WCO biodiesel blend dispersed with nanomaterial on BTE

Brake thermal efficiency (BTE) provides information about how the fuel energy is turned into engine output. The BTE w.r.t. load for pure diesel, WCO biodiesel (B20), and various nanoparticles (CeO_2, MgO, and Al_2O_3) blends, *viz.*, B20C30, B20M30, B20A30, B20C40, B20M40, and B20A40, is discussed in Figure 12. Improvement in BTE is observed as load increases as the enhancement in combustion quality of fuel at higher loads [8, 10, 11, 17]. The inclusion of CeO_2, MgO, and Al_2O_3 nanomaterials in WCO biodiesel for 30 ppm and 40 ppm dosages exhibits an improvement in BTE [11, 13, 17]. Metal nanoparticles improve air-fuel mixing by increasing the surface-to-volume ratio, leading to atomization. This allows for a more efficient fuel reaction with air, which results in enhanced brake thermal efficiency.

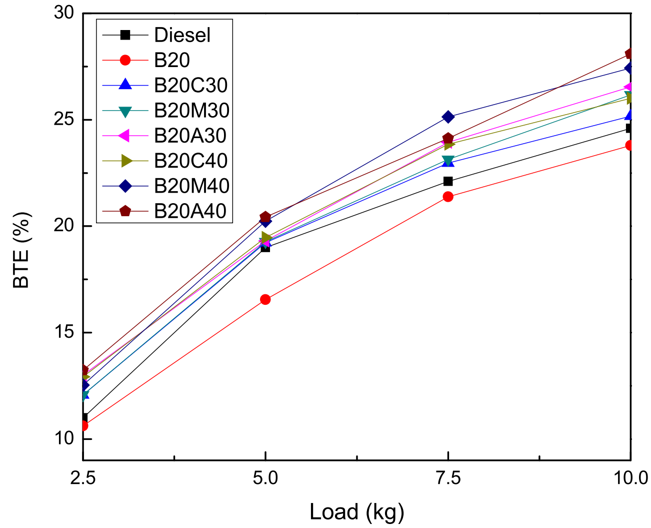

Fig. 12. BTE variation with load for WCO biodiesel mixed with nanomaterials.

3.2 Influence of WCO biodiesel blend dispersed with nanomaterials on SFC

The specific fuel consumption (SFC) w.r.t. load for pure diesel, WCO biodiesel, and various nanoparticles (CeO_2, MgO, and Al_2O_3) blends, *viz.*, B20C30, B20M30, B20A30, B20C40, B20M40, and B20A40, is shown in Figure 13. The decrease in SFC has been seen with enhancement in load because, as load increases, fuel's combustion quality also increases [8, 10, 11, 17]. The SFC is lower for the CeO_2, MgO, and Al_2O_3 nanoparticles mixed in WCO biodiesel (B20) fuel in contrast to neat diesel, which leads to a lower ignition delay and maximizes the surface-to-volume ratio which allows improved combustion and also allows reduced fuel consumption. The mixing of CeO_2, MgO, and Al_2O_3 nanoparticles lowers specific fuel consumption is also seen [11, 13, 17].

3.3 Influence of WCO biodiesel blend dispersed with nanomaterials on η

The mechanical efficiency (η) w.r.t. load for pure diesel, WCO biodiesel, and various nanoparticles (CeO_2, MgO, and Al_2O_3) blends *viz.* B20C30, B20M30, B20A30, B20C40, B20M40, and B20A40 are given in Figure 14. The brake power to the indicated power ratio expressed by the engine is called mechanical efficiency and denoted by. It is improved for improvement in the load (Fig. 14); this is due to enhancement in spray quality and less loss of heat in the blends over the diesel [8, 17]. The mechanical efficiency improved for the CeO_2, MgO, and Al_2O_3 nanoparticles mixed in WCO biodiesel (B20) fuel-diesel comparison [11, 17].

3.4 Influence of WCO biodiesel blend dispersed with nanomaterials on CO

Figure 15 demonstrates the carbon monoxide (CO) w.r.t. load for pure diesel, WCO biodiesel (B20), and various

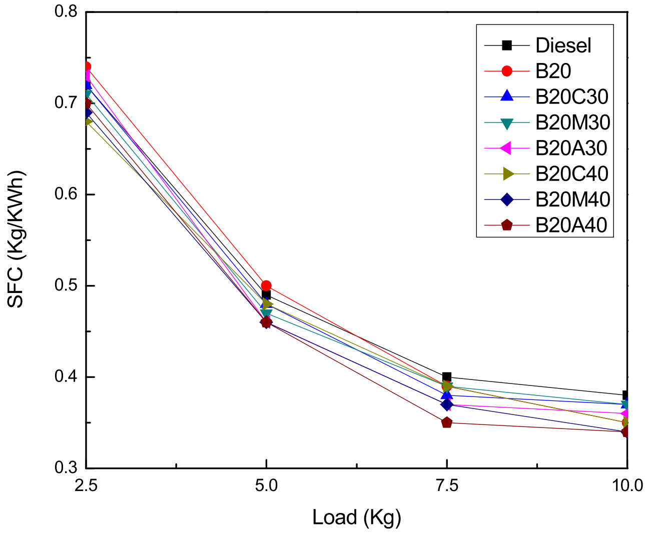

Fig. 13. SFC variation with load for WCO biodiesel mixed with nanomaterials.

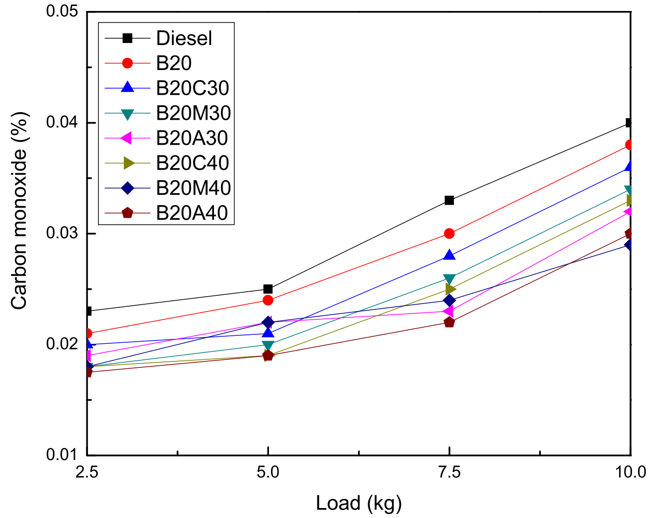

Fig. 15. Carbon monoxide variation with load for WCO biodiesel mixed with nanomaterials.

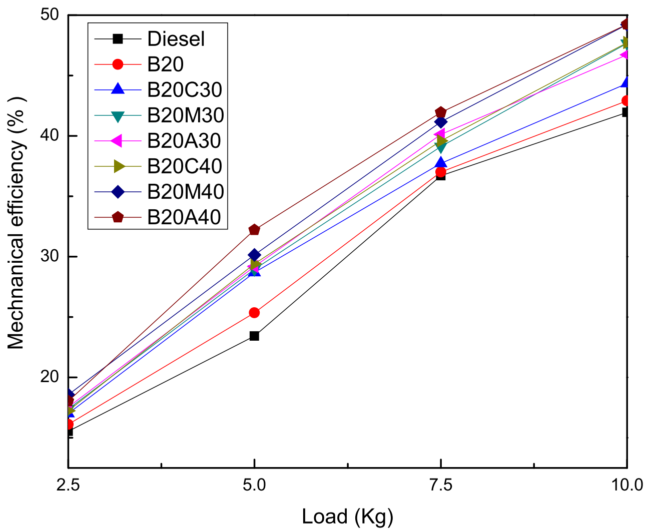

Fig. 14. Mechanical efficiency variation with load for WCO biodiesel mixed with nanomaterials.

nanoparticles (CeO_2, MgO, and Al_2O_3) blends, *viz.*, B20C30, B20M30, B20A30, B20C40, B20M40, and B20A40. It is distinguished from Figure 15 that as the load increases, the increment in CO can be seen for all the mixtures. This is because, at smaller loads, the fuel consumption is less, which gives rise to reduced emissions at higher loads. After all, more fuel consumption leads to higher emissions [9, 15]. The carbon monoxide is reduced for the CeO_2, MgO, and Al_2O_3 nanoparticles mixed in WCO biodiesel (B20) while it is analyzed against the pure diesel. The mixing of nanoparticles supports both the processes (atomization/vaporization) of biodiesel with good mixing of fuel that helps to develop a considerable reduction in CO emissions [15].

3.5 Influence of WCO biodiesel blend dispersed with nanomaterials on HC

The hydrocarbons (HC) w.r.t. load for pure diesel, WCO biodiesel, and various nanoparticles (CeO_2, MgO, and Al_2O_3) blends, *viz.*, B20C30, B20M30, B20A30, B20C40, B20M40, and B20A40, is exhibited in Figure 16. From Figure 16, it is noticed that the HC emissions improved with enhancement in load because of the rich air-fuel mixture and poor oxygen resulting from engine operation [10, 11, 17]. The unburnt hydrocarbons reduced for the CeO_2, MgO, and Al_2O_3 nanomaterials added with WCO biodiesel (B20) fuel over the pure diesel. The addition of nanomaterials to WCO biodiesel fuel reduces unburnt hydrocarbon emissions. This is due to a greater amount of oxygen, which improves the oxidation of hydrocarbons in the biodiesel oil [10, 11].

3.6 Influence of WCO biodiesel blend dispersed with nanomaterials on NO_x

The nitrogen oxides w.r.t. load for pure diesel, WCO biodiesel, various nanoparticles (CeO_2, MgO, and Al_2O_3) blends *viz.*, B20C30, B20M30, B20A30, B20C40, B20M40, and B20A40 are shown in Figure 17. From the illustration of Figure 17, an increase in NO_x emissions is noticed with an increment in the load. This is attributed to an increase in combustion temperature, an increase in the amount of oxygen, and a rapid reaction [10, 11, 13, 17]. In comparison to pure diesel, the WCO biodiesel having CeO_2, MgO, and Al_2O_3 added to it (interaction of nanomaterials with biodiesel air would improve the oxidation process during combustion) enhances the ignition quality of the biodiesel, and as a result, it shows an improvement in the heat release rate that is associated with an increase in the temperature of the exhaust gas, which leads to a higher level of NO_x emissions [11, 13, 17].

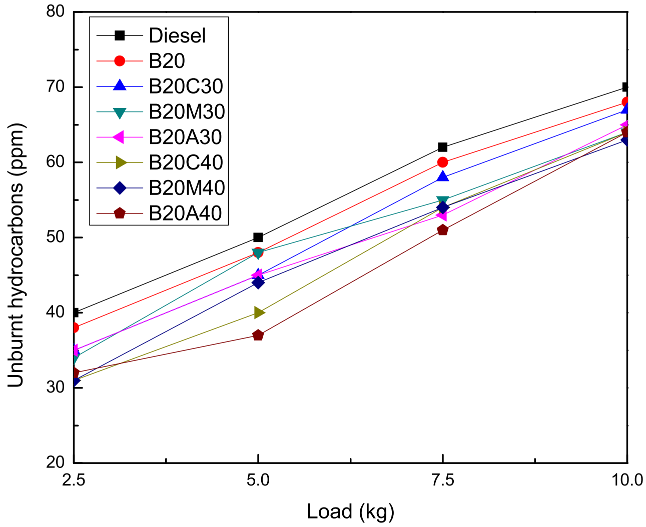

Fig. 16. Hydrocarbons variation with load for WCO biodiesel mixed with nanomaterials.

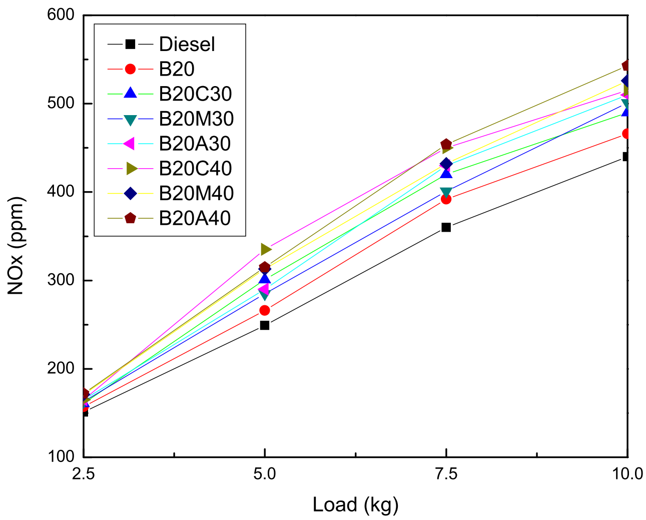

Fig. 17. NO_x variation with load for WCO biodiesel mixed with nanomaterials.

3.7 Influence of WCO biodiesel blend dispersed with nanomaterials on Smoke opacity

Figure 18 presents the smoke opacity w.r.t. load for pure diesel, WCO biodiesel, and various nanoparticles (CeO_2, MgO, and Al_2O_3) blends *viz.*, B20C30, B20M30, B20A30, B20C40, B20M40, B20A40. The increase in smoke opacity that is noticed with a load increment is shown in Figure 18. This is due to the fact of improvement in fuel consumption and the rich air-fuel mixture that is observed [5, 15]. Despite the influence of CeO_2, MgO, and Al_2O_3, there has been a reduction in smoke as a result of a higher surface-to-volume ratio, and there has also been an improvement in ignition qualities [5, 15].

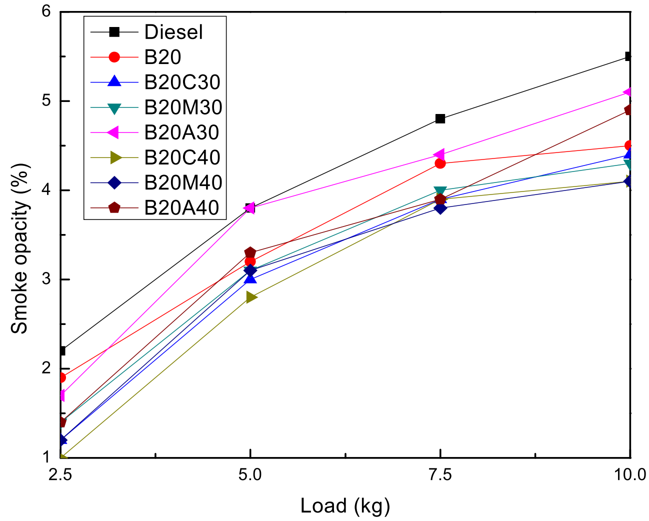

Fig. 18. Smoke opacity variation with load for WCO biodiesel mixed with nanomaterials.

4 Conclusions

In this article, the comparative experimentation on the performance and emissions of a CI engine running with diesel and WCO biodiesel (B20) mixed with Cerium oxide, Magnesium oxide, and Aluminium oxide nanomaterials of 30 ppm and 40 ppm dosages has been done. The subsequent conclusions drawn from the present experimentation are given below:

- The BTE is improved by increasing the addition of nanomaterials, which increases from 24.6% to 26.01%, 27.43%, and 28.1% for B20C40, B20M40, and B20A40, respectively. The SFC decreased by increasing the addition of nanomaterials which decreased from 0.38 kg/KWh to 0.35 kg/KWh, 0.34 kg/KWh, and 0.34 kg/KWh for B20C40, B20M40, and B20A40 respectively. The mechanical efficiency which increases from 41.96% to 47.73%, 49.22%, 49.24%, for B20C40, B20M40, B20A40, respectively (Figs. 12–14).
- The reduction in CO, HC, and Smoke Opacity is observed for increasing the nanomaterials dosage. The CO reduces from 0.04% to 0.032%, 0.033%, and 0.029%, for B20C40, B20M40, B20A40, respectively, HC reduces from 70 ppm to 64 ppm, 63 ppm, 64 ppm, for B20C40, B20M40, and B20A40, respectively, and Smoke Opacity reduced from 5.5% to 4.1%, 4.1%, 4.9%, for B20C40, B20M40, and B20A40, respectively (Figs. 15, 16, 18).
- The nitrogen oxides for Diesel, B20C40, B20M40, and B20A40, are 440 ppm, 515 ppm, 526 ppm, and 543 ppm, respectively (Fig. 17).

In a nutshell, the experimental test results show that the inclusion of cerium oxide (CeO_2), magnesium oxide (MgO), and aluminium oxide (Al_2O_3) nanomaterials at 30 ppm and 40 ppm dosages in 20% WCO nanoparticles improved considerably the performance emission of the CI engine when compared to that of diesel. It is possible to draw the conclusion that adding nanomaterials at higher dosages enhances the CI engine's performance and emissions.

Acknowledgments

The authors further acknowledge "Platonic Nano Tech" Pvt. Ltd., India, and "Nano Research Lab," Jemshedpur, India.

Funding

Vision Group on Science and Technology (VGST), Bengaluru, 560001, Karnataka, India has been supported financially under the scheme "Research Grant for Scientist/Faculty (RGS/F)" (Letter No. KSTePS/VGST/RGS-F/GRDNo.980/2020-21/104, dated-26/08/2021).

References

1 Berenjestanaki A. V., Husain D. (2001) Effect of nitromethane and jatropha biodiesel on the combustion, performance and emission characteristics of diesel engine, *Int. J. Automot. Mech.* **18**, 3, 8986–8997.
2 Hussain S. S., Ali S. A., Bagwan A. H., Husain D., Ahmad A., (2023) Prediction of CI engine emissions fueled with multiwalled carbon nanotube-doped waste cooking oil biodiesel using multilayer neural network, *J. Nanomater.* **2023**, 1, 2508422.
3 Afzal A., Agbulut U., Soudagar M.E.M., Razak R. K., Buradi A., Saleel C. A. (2021) Blends of scum oil methyl ester, alcohols, silver nanoparticles and the operating conditions affecting the diesel engine performance and emission: an optimization study using Dragon fly algorithm, *Appl. Nanosci.* **11**, 9, 2415–2432.
4 Hosamani B. R., Ali S. A., Katti V. (2021) Assessment of performance and exhaust emission quality of different compression ratio engine using two biodiesel mixture: artificial neural network approach, *Alex. Eng. J.* **60**, 1, 837–844.
5 Ranjan A., Dawna S. S., Jayaprabakar J., Nirmala N., Saikiran K., Sai Sriram S. (2018) Experimental investigation on effect of MgO nanoparticles on cold flow properties, performance, emission and combustion characteristics of waste cooking oil biodiesel, *Fuel* **220**, 780–791.
6 Rajak U., Ağbulut Ü., Veza I., Dasore A., Sarıdemir S., Verma T. N. (2022) Numerical and experimental investigation of a CI engine behaviours supported by zinc oxide nanomaterial along with diesel fuel, *Energy* **239**, 122424.
7 Kulkarni M. G., Dalai A. K. (2006) WCOs an economical source for biodiesel: a review, *Ind. Eng. Chem. Res.* **45**, 2901–2913.
8 Ali S. A., Hunagund S., Hussain S. S., Bagwan A. H. (2020) The effect of nanoparticles dispersed in waste cooking oil (WCO) biodiesel on thermal performance characteristics of VCR engine, *Mater. Today: Proc.* **43**, 2, 888–891.
9 Kareemullah M., Afzal A., Fazlur Rehman K., Shahapurkar K., Khan H., Akra N. (2020) Performance and emission analysis of compression ignition engine using biodiesels from Acid oil, Mahua oil, and Castor oil, *Heat. Transf. Res.* **49**, 858–871.
10 Kumar S. S., Rajan K., Mohanvel V., Ravichandran M., Rajendran P., Rashedi A., Sharma A., Khan S. A., Afzal A. (2021) Combustion, performance, and emission behaviors of biodiesel fueled diesel engine with the impact of alumina nanoparticle as an additive, *Sustainability.* **13**, 21, 12103.
11 Ağbulut U., Karagöz M., Sarıdemir M., Öztürk A. (2020) Impact of various metal-oxide based nanoparticles and biodiesel blends on the combustion, performance, emission, vibration and noise characteristics of a CI engine, *Fuel.* **270**, 117521.
12 Lv J., Wang S., Meng B. (2022) The effects of nano-additives added to diesel-biodiesel fuel blends on combustion and emission characteristics of diesel engine: a review, *Energies.* **15**, 1032.
13 Kumar R., Singh B., Arunkumar M., Shan D. P., Patil P. P., Chowdary V.L. (2022) Performance and Emission analysis of waste cooking oil biodiesel mixed with titanium oxide nano-additives, *Int. J. Chem. Eng.* **2022**, 1101771.
14 Prabhu A. (2017) Nanoparticles as additive in biodiesel on the working charecteristics of a DI diesel engine, *Ain. Shams. Eng. J.* **9**, 4, 2343–2349.
15 Gad M. S., Abdel A. M. M., Kayed H. (2022) Impact of different nano additives on performance, combustion, emissions and exergetic analysis of a diesel engine using waste cooking oil biodiesel, *Propuls. Power. Res.* **11**, 2, 209–223.
16 Abed K. A., El Morsi A. I., Sayed M. M., El Shaib A. A., Gad M. S. (2018) Effect of waste cooking-oil biodiesel on performance and exhaust emissions of a diesel engine, *Egypt. J. Pet.* **27**, 4, 985–989.
17 Padmanabhan S., Selvamuthukumar M., Mahalingam S., Giridharan K., Ganesan S. (2023) Influential study of oxygenated additives in waste cooking biodiesel blends on diesel engine performance, *Multidiscip. Sci. J.* **5**, 2, 2023015.
18 Tamrat S., Ancha V. R., Gopal R., Nallamothu R. B., Seifu Y. (2024) Emission and performance analysis of diesel engine running with CeO_2 nanoparticle additive blended into castor oil biodiesel as a substitute fuel, *Sci. Rep.* **14**, 1, 7634.
19 Çalık A., Tosun E., Akar M. A., Özcanlı M. (2023) Combined effects of hydrogen and TiO_2 nanoparticle additive on terebinth oil biodiesel operated diesel engine, *Sci. Tech. Energ. Transition* **78**, 9. https://doi.org/10.2516/stet/2023007.
20 Rajeswari K. T., Selvadas S. S. R. (2023) Performance and emission characteristics of salviniaceae filiculoides aquatic fern oil and SiO_2 nano additive biodiesel in CI engine, *Sci. Tech. Energ. Transition* **78**, 4. https://doi.org/10.2516/stet/2022021.
21 Thanikodi S., Rangappa S. M., Sebayang A. H., Siengchin S. (2023) Performance of IC engines using chicken waste as biofuel, CNT and MnO nano-biofuels and diesel fuel: a comparation study, *Automot. Exp.* **6**, 2, 395–406. https://doi.org/10.31603/ae.9556.
22 Yilbaşi Z., Yesilyurt M. K., Yaman H., Arslan M. (2022) The industrial-grade hemp (*Cannabis sativa* L.) seed oil biodiesel application in a diesel engine: combustion, harmful pollutants, and performance characteristics, *Sci. Tech. Energ. Transition* **77**, 15. https://doi.org/10.2516/stet/2022011.
23 Yaman H., Saltan G., Doğan B., Yeşilyurt M. K., Sarıkoç S. (2023) Examination of a CI engine running on poppy seed oil biodiesel/n-pentanol/diesel fuel blends with respect of thermodynamic and economic perspectives, *Sci. Tech. Energ. Transition* **78**, 40. https://doi.org/10.2516/stet/2023040.
24 Soudagar M. E. M., Shelare S., Marghade D., Belkhode P., Nur-E-Alam M., Kiong T. S., Ramesh S., Rajabi A., Venu H., Khan T. Y., Mujtaba M., Shahapurkar K., Kalam M., Fattah I. (2024) Optimizing IC engine efficiency: a comprehensive review on biodiesel, nanofluid, and the role of artificial intelligence and machine learning, *Energy Convers.*

Manag. **307**, 118337. https://doi.org/10.1016/j.enconman.2024.118337.

25 Awogbemi O., Onuh E. I., Inambao F. L. (2019) Comparative study of properties and fatty acid composition of some neat vegetable oils and waste cooking oils, *Int. J. Low. Carbon. Technol.* **14**, 3, 417–425.

26 Zhang D., Cao C. Y., Lu S., Cheng Y., Zhang H. P. (2019) Experimental insight into catalytic mechanism of transition metal oxide nanoparticles on combustion of 5-Amino-1H-Tetrazole energetic propellant by multi kinetics methods and TG-FTIR-MS analysis, *Fuel* **245**, 78–88. https://doi.org/10.1016/j.fuel.2019.02.007.

27 Manigandan S., Sarweswaran R., Devi P. B., Sohret Y., Kondratiev A., Venkatesh S., Vimal M. R., Joshua J. J. (2020) Comparative study of nanoadditives TiO_2, CNT, Al_2O_3, CuO and CeO_2 on reduction of diesel engine emission operating on hydrogen fuel blends, *Fuel* **262**, 116336. https://doi.org/10.1016/j.fuel.2019.116336.

28 Mei D., Li X., Wu Q., Sun P. (2016) Role of cerium oxide nanoparticles as diesel additives in combustion efficiency improvements and emission reduction, *J. Energy Eng.* **142**, 4, 04015050. https://doi.org/10.1061/(asce)ey.1943-7897.0000329.

29 Kumar Y., Yogeshwar P., Bajpai S., Jaiswal P., Yadav S., Pathak D. P., Sonker M., Tiwary S. K. (2021) Nanomaterials: stimulants for biofuels and renewables, yield and energy optimization, *Mater. Adv.* **2**, 16, 5318–5343. https://doi.org/10.1039/d1ma00538c.

30 El-Seesy A. I., Attia A. M., El-Batsh H. M. (2018) The effect of Aluminum oxide nanoparticles addition with Jojoba methyl ester-diesel fuel blend on a diesel engine performance, combustion and emission characteristics, *Fuel* **224**, 147–166. https://doi.org/10.1016/j.fuel.2018.03.076.

31 Yusof S. N. A., Sidik N. A. C., Asako Y., Japar W. M. A. A., Mohamed S. B., Muhammad N. M. A. (2020) A comprehensive review of the influences of nanoparticles as a fuel additive in an internal combustion engine (ICE), *Nanotechnol. Rev.* **9**, 1, 1326–1349.

32 Ruan B., Jacobi A. M. (2012) Ultrasonication effects on thermal and rheological properties of carbon nanotube suspensions, *Nanoscale Res. Lett.* **7**, 1, 127. https://doi.org/10.1186/1556-276x-7-127.